JTE HCMUTE
ISSN: 2615-9740

JOURNAL OF TECHNICAL EDUCATION SCIENCE
Ho Chi Minh City University of Technology and Education
Website: https://jte.edu.vn
Email: jte@hcmute.edu.vn

R152a and R134a: High-Performance Working Fluids for Ejector Cooling Systems

Van Vu Nguyen[*1], **Yevgeniy Muralev**[2]
[1]*Ho Chi Minh City University of Technology and Education, Vietnam*
[2]*Caspian University of Technology and Engineering, Kazakhstan*

[*]Corresponding author. *Email: nguyenvanvu@hcmute.edu.vn*

ARTICLE INFO

Received: 05/06/2025
Revised: 01/07/2025
Accepted: 23/07/2025
Published: 28/11/2025

KEYWORDS

R600a;
HFOs;
Ejector refrigeration;
EES;
R152a.

ABSTRACT

This study presents a comprehensive thermodynamic analysis of an ejector cooling system (ECS) using a detailed one-dimensional mathematical model implemented in Engineering Equation Solver (EES) software. The research investigates the impact of key operational parameters such as secondary flow superheating, generator temperature, and primary nozzle superheat on system performance, specifically the entrainment ratio (ER) and coefficient of performance (COP). A comparative assessment of five working fluids (R134a, R152a, R600a, R1234ze(E), and R1233zd(E)) was conducted. Results indicate that secondary flow superheating generally enhances COP with minimal ER impact, while increased generator temperature improves both ER and COP. Primary nozzle superheat proved critical for overall performance. Among the investigated refrigerants, R134a and R152a demonstrated the highest COP. Notably, the low-GWP refrigerants R600a and R1234ze(E) showed promising and competitive performance, highlighting their potential as environmentally friendlier alternatives in heat-driven ejector cooling applications. The developed model serves as a robust tool for designing and analyzing ejector cooling systems.

Doi: https://doi.org/10.54644/jte.2025.1915

1. Introduction

Air conditioning of indoor spaces is essential for human well-being and productivity in hot and humid regions globally. Lee Kuan Yew, the first Prime Minister of Singapore, noted in his biography [1] that Space cooling demand is rapidly increasing due to economic growth and climate change. Nowadays, 99% of private dwellings in Singapore are equipped with air conditioners, which operate for most of the time the apartment is. In contrast, only 4% of households in India possess an air conditioner, despite significant cooling needs.

Cooling indoor environments is vital for comfort and productivity, particularly in hot and humid climates around the world. In his memoir, Singapore's founding Prime Minister, Lee Kuan Yew, emphasized the transformative role of air conditioning in modern life [1]. Driven by economic development and the impacts of climate change, global demand for space cooling is rising sharply. In Singapore, air conditioners are now installed in 99% of private homes and are used extensively whenever residents are present [1]. Conversely, in India—despite facing substantial cooling requirements—only 4% of households have access to air conditioning [2].

Approximately 1.6 billion air conditioners are in use worldwide, with the highest concentrations in China, USA. Rising economic development in emerging economies, combined with the effects of global warming, is expected to drive a substantial surge in demand for air conditioning. For example, the number of air conditioning units in use in India is projected to grow from approximately 30 million in 2016 to over 1 billion by 2050 [3]. Electricity use for space cooling is rapidly emerging as the dominant

component of energy consumption in buildings, as illustrated in Figure 1. Projections suggest that by 2050, around 5.6 billion air conditioning units will be in operation worldwide. At current efficiency levels, these systems are expected to consume approximately 6,200 terawatt-hours of electricity annually, accounting for nearly 30% of total building electricity demand (see Figure 1). As a result, air conditioning is becoming a significant driver of global carbon dioxide emissions.

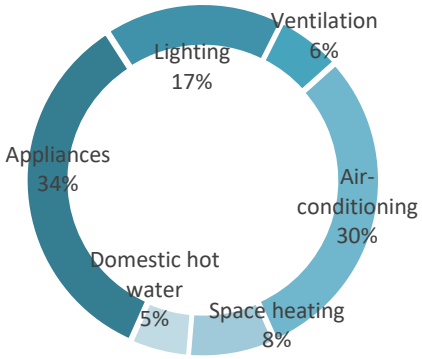

Figure 1. *Building electricity consumption by 2050, extracted from IEA [2]*

Air conditioning alone is projected to account for a 0.5°C increase in global temperatures [4] within the broader expected rise of 3 to 5°C by the end of this century. The combustion of fossil fuels releases carbon dioxide, intensifying the greenhouse effect and driving unsustainable climate change. Its consequences are increasingly visible through rising sea levels and a surge in extreme weather events, including floods and severe storms. A heat-driven cooling system, such as ejector refrigeration can be a great substitute for conventional air conditioning systems in the near future. A key advantage of ejector cooling systems is their ability to utilize low-grade thermal energy instead of electricity.

The ejector is a key component in a heat-driven cooling cycle that replaces the traditional compressor with a jet-based mechanism and no moving parts. It uses high-pressure vapor from a generator (the primary stream), which accelerates through a nozzle to create a low-pressure zone. This draws in lower-pressure vapor from the evaporator (the secondary stream), and the two streams mix inside the ejector. As the combined flow slows down in the diffuser section, its pressure increases, effectively compressing the refrigerant. This fluid-dynamic process enables cooling using heat sources like solar or waste heat, making the ejector both simple and energy-efficient.

2. Literature review

Refrigerants R134a and R152a are prominent HFC refrigerants favored for Ejector Refrigeration Systems (ERS) due to their high performance across various ERS technologies [4], [5], [6]. R134a has been widely adopted in the refrigeration industry owing to its excellent thermal performance[7], [8], [9], [10]. However, its high Global Warming Potential (GWP) has led to its phasing out under recent regulations.

Hydrochlorofluorocarbons and hydrofluorocarbons have been widely used in ejector refrigeration systems (ERS) due to their favorable thermodynamic properties and relatively high performance. Among HFCs, R134a, R410a, R245fa, and R407c are the most commonly employed refrigerants in both experimental research and practical applications. For example, R134a has been used in theoretical studies by Khalil et al. [4] and in experimental investigations by Yan et al. [5], while R245fa was adopted in the experimental work of Huang et al. [6].

However, the widespread use of HCFCs and high-GWP HFCs has raised significant environmental concerns, particularly regarding their ozone depletion potential (ODP) and global warming potential (GWP). As a result, many of these substances are being gradually phased out or banned under international agreements and regional regulations, such as the European Union’s Regulation 517/2014 [10], which limits the use of high-GWP refrigerants.

Direct emissions of refrigerants used as working fluids in cooling systems significantly contribute to climate change. To address this issue, European Regulation (EU) No. 517/2014 [11] denoted that from January 2022, new commercial refrigeration units must not use refrigerants with a global warming potential (GWP) of 150 or higher. This regulation presents a major challenge, as many widely used refrigerants far exceed this value. For example, R134a (GWP 1430) and the HFC blend R410a (GWP 2088).

Among commonly used HFCs, R152a stands out as the most favorable for ERS applications. R152a (GWP of 138) presents a more environmentally friendly option. It has demonstrated comparable or even superior performance to R134a under similar operating conditions [12]. Both R134a and R152a are wet refrigerants, which means they require a certain degree of superheat at the ejector inlets to avoid condensation and ensure efficient mixing and entrainment (see ***Table 1***).

Hydrofluoroolefins (HFOs) are the fourth generation of halogen refrigerants, boasting zero Ozone Depletion Potential (ODP) and exceptionally low Global Warming Potential (GWP) values. Despite their environmental benefits, the commercial availability of certain HFOs, like R1234ze(e), is still not very common. This limited accessibility is reflected in the scarcity of published research on ejector refrigeration systems employing HFOs as working fluids.

Table 1. *Working fluids used in ejector refrigeration system in literature.*

Refrigerant	T_g *(°C)*	T_c *(°C)*	T_e *(°C)*	ΔT_{sup} *(K)*	***COP*** *(-)*	***Cooling Capacity*** *[kW]*
R718 *[13]*	40-70	12-32	10	-	0.18-0.27	up to 0.7
R600a *[14]*, *[15]*	87	29	6	5-15	0.2-0.31	1-2
R113 *[16]*	65-100	42-50	5-18	-	0.1-0.2	-
R134a *[17]*	72-78	31	10	-	0.1-0.35	0.25-1.3
R152a *[4]*	70-100	25-35	5-15	5	0.35-0.75	1
R245fa *[18]*	80-105	24-42	4-20	5-7	0.25-0.45	4-7
R141b *[19]*	90-100	30-32	6-8	-	0.5-0.6	10.5

Ejector refrigeration has been explored with various refrigerants (including R134a, R600a) and forth generation of Halocarbons. The current work emphasizes the influences of the refrigerant used in the system. Our model integrates advanced sub-models and real-gas data to address these gaps.

3. Mathematical modeling

The mathematical model was developed using Engineering Equation Solver (EES), a software tool specialized in solving both linear and nonlinear systems of algebraic and differential equations. One of EES's key strengths is its flexibility in handling equations in any sequence input, without affecting the outcome, a capability that sets it apart from many other engineering programs. Additionally, EES offers a comprehensive and highly accurate built-in database that provides thermodynamic and transport properties for a wide range of substances [20]

3.1. Model assumptions

The mathematical model is based on the following assumptions to ensure a balance between computational simplicity and accuracy:

- Steady-state operation: all thermodynamic processes and flow properties (mass flow rate, pressure, temperature…) are assumed constant with time.
- One-dimensional flow: the flow is considered along a single spatial dimension, with cross-sectional properties uniform at any given section.

- Adiabatic flow: heat transfer to or from the ejector walls is neglected, assuming adiabatic operation.
- Normal shock wave: a normal shock is assumed to occur in the ejector mixing section, facilitating conversion from supersonic to subsonic flow.
- Isentropic efficiencies: each component (nozzle, mixing section, diffuser) is modeled using fixed isentropic efficiencies based on literature values.

3.2. Governing equation

The mathematical model for the ejector cooling cycle is founded on the fundamental thermodynamic conservation principles of mass, energy, and momentum. To improve the model's precision, the heat exchanger components incorporate subcooling of the liquid refrigerant at the condenser exit and superheating of the vapor at the outlets of both the generator and evaporator. These enhancements are based on findings from our earlier studies [21], [22].

This mathematical model is implemented using EES, which is integrated real-gas database. Thus, the software can supply the necessary thermodynamic and transport properties for the working fluids. This database is particularly critical for modeling the ejector, as its internal flow conditions are characterized by supersonic speeds, the presence of shock waves, and high compressibility. Those features are crucial for the mathematical model to achieve accurate results.

3.2.1. System performance indicator

Coefficient of performance (COP) represents the cooling effect produced in the evaporator relative to the heat energy consumed in the generator. Therefore, a higher entrainment ratio, along with a greater enthalpy change (heat absorption) in the evaporator compared to the enthalpy change (heat input) in the generator, will result in a higher COP and a more efficient system. This enthalpy difference ratio specifically compares the enthalpy change from the evaporator outlet (after the expansion valve) to the enthalpy change from the generator outlet (after the pump), as detailed in the following mathematical expression:

$$COP \cong \frac{\dot{m}_e \cdot (h_e - h_v)}{\dot{m}_g \cdot (h_g - h_p)} = ER \frac{(h_e - h_v)}{(h_g - h_p)} \quad (1)$$

Where $(h_e - h_v)$ is the specific cooling capacity; $(h_g - h_p)$ represents the specific heat absorbed by the refrigerant at the generator.

3.2.2. Equation formulation

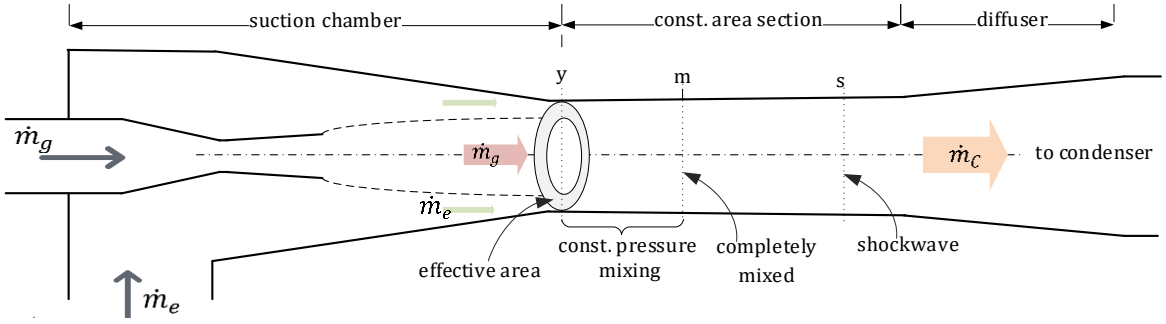

Figure 2. *Working schematic of the ejector.*

Figure 2 presents a schematic of an ejector, divided into three theoretical sections: the suction chamber, constant-area mixing section, and diffuser. The primary flow ($\dot{m}_g$) entrains the secondary flow ($\dot{m}_e$) from the suction chamber. Mixing occurs under constant pressure conditions, followed by complete mixing and a normal shock wave. The mixed flow $\dot{m}_c$ is then compressed in the diffuser before

being discharged to the condenser. The theoretical model is built based on the conservation laws of mass, energy and momentum of the ejector.

Under choked flow conditions, where the fluid velocity at the nozzle throat reaches the speed of sound, the primary mass flow rate is at its maximum. This rate is defined by the following equation from ideal gas dynamics:

$$\dot{m}_g = A_t \frac{p_g}{\sqrt{T_g + T_{sup}}} \sqrt{\eta_t \frac{\kappa}{R} \left(\frac{2}{\kappa + 1} \right)^{\frac{\kappa+1}{\kappa-1}}} \tag{2}$$

Where p_g is the primary inlet pressure, T_g is the saturation temperature at pressure p_g and T_{sup} is the degree of superheat in the primary flow.

In equation (2), η_t denotes the primary nozzle's isentropic efficiency. κ and R refer to the heat capacity ratio and the gas constant for the specific refrigerant used.

The nozzle outlet area (A_{NO}) and throat area (A_t) (see ***Figure 2***) are determined using the following equation:

$$A_{NO} = (A_t / Ma_{NO}) \left[\frac{2}{\kappa + 1} \left(1 + \frac{\kappa - 1}{2} Ma_{NO}^2 \right) \right]^{\left(\frac{\kappa+1}{\kappa-1}\right)/2} \tag{3}$$

The pressure at the nozzle outlet is a function of the primary inlet pressure and the nozzle outlet Mach number ($\mathrm{M}a_{NO}$), as defined by the following equation:

$$p_{NO} = p_g \left(1 + \frac{\kappa - 1}{2} Ma_{NO}^2 \right)^{\frac{-\kappa}{\kappa-1}} \tag{4}$$

Therefore, it can be obtained for a given working fluid by the pressure at the secondary inlet of the ejector (p_e) corresponds to the saturation condition and can thus be determined for a given working fluid using:

$$p_e = f(T_{e,sat}) \tag{5}$$

At critical operating mode, the secondary flow at the hypothetical throat (Figure 2) is assumed to be choked [23]:

$$Ma_{e2} = 1 \tag{6}$$

The pressure of the secondary flow at the hypothetical throat (p_{e2}) can be determined using the following expression:

$$p_{e2} = p_e \left(1 + \frac{\kappa - 1}{2} Ma_{e2}^2 \right)^{\frac{-\kappa}{\kappa-1}} \tag{7}$$

Under the constant-pressure mixing assumption, we consider the pressures of the primary and secondary fluids to be equal where they combine at the hypothetical throat [23]. This allows the cross-sectional area occupied by the primary flow (A_{g2}) at section 2 to be calculated with the following isentropic relation:

$$A_{g2} = \frac{\phi_p \, A_t}{Ma_{g2}} \left[\frac{2}{\kappa + 1} \left(1 + \frac{\kappa - 1}{2} Ma_{g2}^2 \right) \right]^{\left(\frac{\kappa+1}{\kappa-1}\right)/2} \tag{8}$$

In equation (8), the secondary mass flow rate is calculated based on the required cooling capacity ($\dot{Q}_e$), which is a key input for the model. This equation incorporates the Mach number of the primary stream at the constant area section ($\mathrm{M}a_{g2}$), and the efficiency of the primary flow from the nozzle outlet to the hypothetical section (ϕ_p) as follows:

$$\dot{m}_e = \frac{\dot{Q}_e}{(h_e - h_v)} \tag{9}$$

In equation (9), h_e represents the enthalpy at the evaporator outlet, while h_v denotes the enthalpy at the expansion valve outlet.

Assuming choked flow, the hypothetical cross-sectional area of the secondary stream A_{e2}can be calculated using the following expression:

$$\dot{m}_e = A_{e2} \frac{p_e}{\sqrt{T_e + T_{sup,e}}} \sqrt{\eta_e \frac{\kappa}{R} \left(\frac{2}{\kappa + 1}\right)^{\frac{\kappa+1}{\kappa-1}}} \tag{10}$$

In equation (10), T_e denotes the saturation temperature of the refrigerant, while $T_{sup,e}$ represents the applied superheat degree. The primary flow temperature at section 2 can be calculated from the primary inlet temperature using the following expression:

$$T_{g2} = \frac{T_g + T_{sup}}{1 + \frac{\kappa - 1}{2} Ma_{g2}^2} \tag{11}$$

The flow velocities at the hypothetical throat can be obtained using the two following expression:

$$v_{g2} = Ma_{g2} \sqrt{\kappa \; R \; T_{g2}} \tag{12}$$

$$v_{e2} = Ma_{e2} \sqrt{\kappa \; R \; T_{e2}} \quad . \tag{13}$$

The mixing occurs within the constant area section (***Figure 2)*** under constant pressure, where the kinetic energy from the primary flow transfers to the secondary flow. The mixing is considered complete at section 3. The velocity of the mixed flow (v_3) is determined using the relation presented in [24]:

$$v_3 = \left(v_{g2} + ER \; v_{e2}\right) \frac{\sqrt{\phi_3}}{1 + ER} \tag{14}$$

The Mach number at section 3 is calculated as follows, where Φ_3 represents the isentropic efficiency of the mixing process:

$$Ma_3 = \frac{v_3}{\sqrt{\kappa \; R \; T_3}} \tag{15}$$

The temperature of mixed flow (T_3) is obtained by applying the energy balance between section *2* and *3*:

$$\left(\dot{m}_g + \dot{m}_e\right) \left(T_3 \; c_{p_3} + \frac{v_3^2}{2}\right) = \dot{m}_g \left(T_{g2} \; c_{p_{g2}} + \frac{v_{g2}^2}{2}\right) + \dot{m}_e \left(T_{e2} \; c_{p_{e2}} + \frac{v_{e2}^2}{2}\right). \tag{16}$$

It is assumed that a normal shock wave occurs between sections 3 and 4 of the mixed flow (constant area section). This shock wave is idealized as taking place over an infinitesimally short segment of the ejector, resulting in abrupt changes in fluid properties, including pressure, temperature, velocity, and density. The relationship between the static pressures before and after the shock wave, denoted as p_3 and p_4, is given by:

$$p_4 = p_{g2} \left(1 + \frac{2}{\kappa + 1} \kappa \left(Ma_3^2 - 1\right)\right) \tag{17}$$

In equation (17) it is considered that $p_3 = p_{g2}$, then the Mach number after the shockwave $\mathrm{M}a_4$ is:

$$Ma_4 = \sqrt{\frac{1 + \frac{\kappa - 1}{2} Ma_3^2}{\kappa\, Ma_3^2 - \frac{\kappa - 1}{2}}} \tag{18}$$

The mixed flow through the diffuser undergoes an isentropic process, characterized by an isentropic efficiency of the diffuser section η_D , the exit pressure p_D can be expressed as:

$$p_D = p_4 \left(1 + \eta_D \frac{\kappa - 1}{2} Ma_4^2\right)^{\frac{\kappa}{\kappa - 1}} \tag{19}$$

4. Results and Discussion

The study aimed to evaluate common use in the refrigeration industry and emerging options suitable for ejector cooling systems. The reasons for these specific choices included high performance Hydrofluorocarbon (HFC) refrigerants R134a and R152a due to their widespread use; the natural refrigerant R600a (isobutane) was included because of its excellent thermodynamic properties and low GWP. New generation Hydrofluoroolefins (HFOs) with very low GWP, R1234yf, and R1233zd(E), were also considered to assess environmentally friendlier, and are potential alternatives to HFCs.

4.1. Superheat of the secondary inlet flow

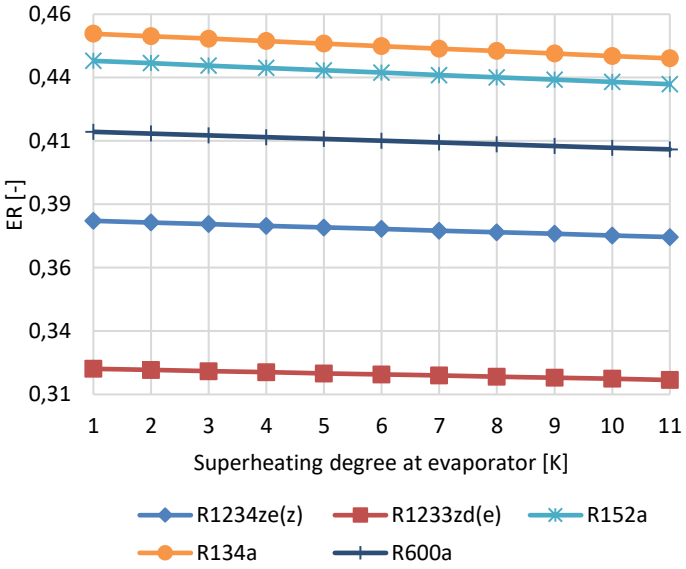

Figure 3. *Entrainment ratio as a function of* $\boldsymbol{\Delta T_{sh,e}}$.

Figure 3 presents the effect of secondary flow superheating on the ejector entrainment ratio (ER). Across the full superheating range (1 to 11 K), the ERs of the selected refrigerants show only a slight decrease. As with the previous case, the variation in ERs with respect to $\Delta T_{sh,e}$ can be explained using Equation 1. Compared to the ER variations caused by $\Delta T_{sh,g}$, the changes in ERs due to $\Delta T_{sh,e}$ are more uniform across all refrigerants. The ER curves are mostly parallel, with no irregular behavior observed for R1234yf and R134a, unlike in the previous analysis.

This suggests that superheating at the inlet causes only minor changes in entrainment performance. The extent of ER variation depends on both the refrigerant type and operating temperature. For example, more noticeable ER fluctuations occur at higher operating temperatures, whereas variations are minimal at lower secondary flow inlet temperatures.

Figure 4 demonstrates the impact of secondary inlet flow superheating on overall system performance. Unlike the entrainment ratio, the coefficient of performance (COP) shows significant sensitivity to variations in superheating. As seen in the figure, increasing the superheat leads to improved system performance. This trend can be explained by the COP formulation: as the degree of superheating increases, the specific enthalpy of the secondary inlet flow rises accordingly. Since the enthalpy difference Δh_e is directly proportional to the COP, an increase in superheat results in a higher COP.

Furthermore, as previously discussed, the change in secondary mass flow rate with respect to $\Delta T_{sh,e}$ is minimal. Therefore, the positive effect of superheating on COP remains dominant, confirming that elevated superheat at the secondary inlet enhances system performance.

This observation aligns with findings from earlier experimental studies [22], [25] which reported that superheating in the secondary inlet flow is commonly present. Due to the suction mechanism pulling refrigerant from the evaporator to the ejector inlet, a vacuum region forms, naturally inducing a degree of superheating. In the experimental investigation conducted for this thesis, the superheat at the secondary inlet was found to range from approximately 2 to 7 K.

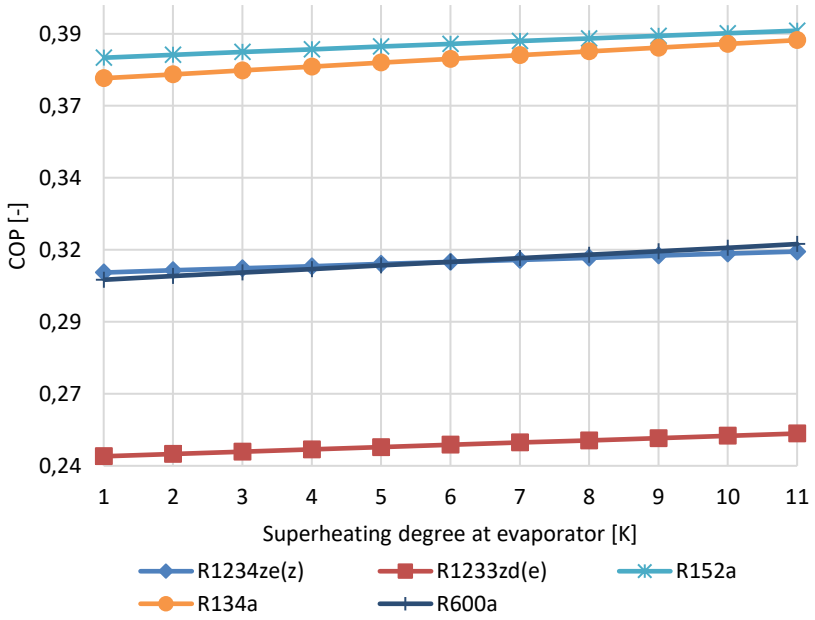

Figure 4. *Coefficient of performance as a function of* $\boldsymbol{\Delta T_{sh,e}}$.

4.2. Coefficient of performance as a function of the generator temperature

Figure 5 provides a comparative overview of the coefficient of performance (COP for seven distinct working fluids. The performance of these refrigerants was evaluated under uniform operating conditions: a generator temperature (T_g) of 90°C, a condenser temperature (T_c) of 35°C, an evaporator temperature (T_e) of 10°C.

R152a and R134a demonstrate the most superior performance, achieving the highest COP among all refrigerants tested. Which is primarily because of advantageous thermodynamic properties of R152a, such as suitable latent heat and specific heat capacity values, which positively contribute to both the ejector's operational effectiveness and the overall cycle efficiency under these specific conditions. Following R152a and R134a, R600a and HFO R1234ze(z) also exhibit notable high COP values. R600a and R1234ze(z) are competitive COP profiles when compared against the other common working fluids.

Moreover, these two refrigerants are environmentally friendly (low GWP), making them great alternatives, suitable for this thermal-driven cooling technology. Conversely, HFO R1233zd(e) records lower COP values in this comparison, thus it is not suitable for ejector cooling applications in terms of thermodynamics performance.

Compared with entrainment ratios shown in ***Figure 4,*** higher entrainment ratios also tend to yield higher coefficients of performance. This correlation is expected, as a higher ER signifies a greater mass flow rate of the secondary fluid (from the evaporator) per unit mass of the primary fluid, which typically translates to an increased cooling capacity. Nevertheless, the COP is not solely dictated by the ER; it is also significantly influenced by other specific thermodynamic properties of each refrigerant that affect the required heat input in the generator and the overall energy balance within the refrigeration cycle.

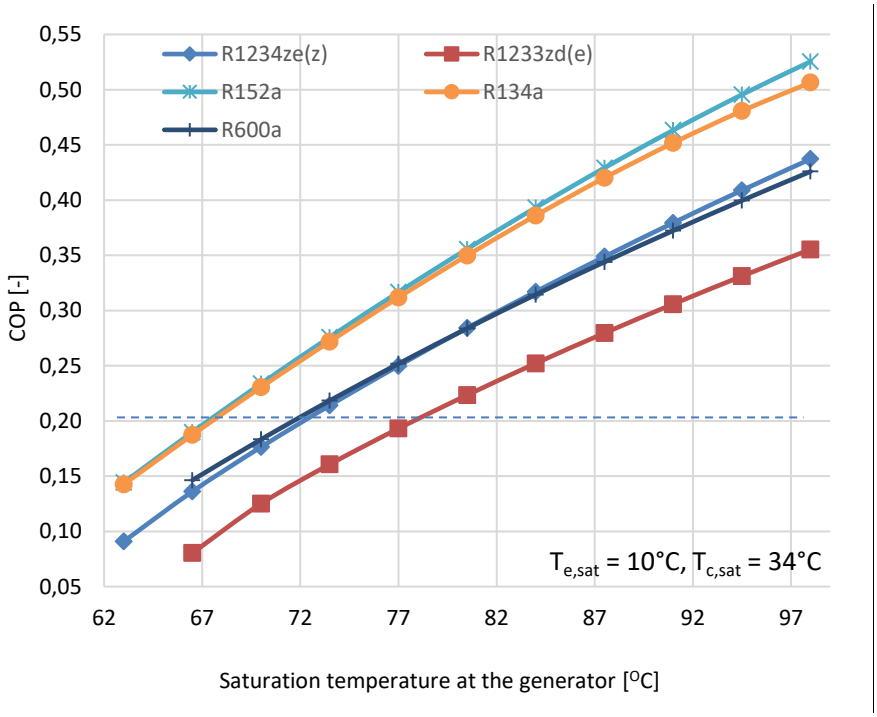

Figure 5. *COP as a function of the saturation at the generator.*

5. Conclusions

This study presented a comprehensive theoretical investigation into the thermodynamic performance of ejector cooling system. A detailed one-dimensional mathematical model of the ejector, for the primary nozzle, mixing chamber, and diffuser was developed and implemented within the EES software. mathematical model developed in this study serves as a valuable and robust tool for the design and analysis of ejector cooling systems.

Parametric analysis revealed that secondary flow superheating ($\Delta T_{sh,e}$) exerts a positive influence on the COP, generally enhancing it while having a minimal impact on the entrainment ratio. However, further increase $\Delta T_{sh,e}$ has negative impact on the system performance. An increase in the generator temperature (T_g) was typically found to improve both ER and COP, signifying enhanced system efficacy at higher heat source temperatures congruent with solar thermal energy inputs. Primary nozzle superheat was identified as a critical parameter, significantly affecting both ER and COP, thus underscoring its importance in the optimization of system performance.

A comparative assessment of 5 selected working fluids (R134a, R152a, R600a, R1234ze(E) and R1233zd(E)) was conducted. Under the specified operating conditions, R134a and R152a demonstrated the highest COP, making them highly favorable working fluids. R1234ze(z), showed promising and

competitive performance, with COP values comparable to environmentally friendly R600a. This highlights their potential as effective, low-GWP alternatives in ejector cooling applications.

Acknowledgments

The authors gratefully acknowledge the Ho Chi Minh City University of Technology and Education for the support by the Project No. T2024-43 and technical support from Caspian University of Technology and Engineering.

Conflict of Interest

The authors declare no conflict of interest.

Data Availability Statement

The data that support the findings of this study are available from the corresponding author upon reasonable request.

REFERENCES

[1] G. Happle, E. Wilhelm, J. A. Fonseca, and A. Schlueter, "Determining air-conditioning usage patterns in Singapore from distributed, portable sensors," *Energy Procedia*, vol. 122, pp. 313–318, Sep. 2017, doi: 10.1016/j.egypro.2017.07.328.
[2] OECD/IEA, *The Future of Cooling: Opportunities for Energy-Efficient Air Conditioning*, Paris, France: IEA, 2018.
[3] V. Mohan, "India's share in global air conditioning units to jump from 2.2% to almost 25% by 2050." [Online]. Available: https://economictimes.indiatimes.com/news/environment/global-warming/indias-share-in-global-air-conditioning-units-to-jump-from-2-2-to-almost-25-by-2050/articleshow/66595350.cms
[4] R. Roman and J. I. Hernandez, "Performance of ejector cooling systems using low ecological impact refrigerants," *Int. J. Refrig.*, vol. 34, no. 7, pp. 1707–1716, 2011, doi: 10.1016/j.ijrefrig.2011.03.006.
[5] G. Besagni, R. Mereu, G. Di Leo, and F. Inzoli, "A study of working fluids for heat driven ejector refrigeration using lumped parameter models," *Int. J. Refrig.*, vol. 58, pp. 154–171, 2015, doi: 10.1016/j.ijrefrig.2015.06.015.
[6] G. Besagni, R. Mereu, and F. Inzoli, "Ejector refrigeration: A comprehensive review," *Renew. Sustain. Energy Rev.*, vol. 53, pp. 373–407, Jan. 2016, doi: 10.1016/j.rser.2015.08.059.
[7] Y. L. Li *et al.*, "Investigation on the effect of ejector liquid recirculation system on the performance of falling-film water chiller with R134a," *Int. J. Refrig.*, vol. 74, pp. 333–344, 2017, doi: 10.1016/j.ijrefrig.2016.11.009.
[8] J. Yan *et al.*, "Experimental study on key geometric parameters of an R134A ejector cooling system," *Int. J. Refrig.*, vol. 67, pp. 102–108, 2016, doi: 10.1016/j.ijrefrig.2016.04.001.
[9] J. Yan, W. Cai, and Y. Li, "Geometry parameters effect for air-cooled ejector cooling systems with R134a refrigerant," *Renew. Energy*, vol. 46, pp. 155–163, 2012, doi: 10.1016/j.renene.2012.03.031.
[10] J. Yu, Y. Ren, H. Chen, and Y. Li, "Applying mechanical subcooling to ejector refrigeration cycle for improving the coefficient of performance," *Energy Convers. Manag.*, vol. 48, no. 4, pp. 1193–1199, 2007, doi: 10.1016/j.enconman.2006.10.009.
[11] The European Parliament, "Regulation (EU) no 517/2014 of the European Parliament and of the Council," 2014. [Online]. Available: https://eur-lex.europa.eu/legal-content/EN/TXT/?uri=CELEX%3A32014R0517
[12] S. Varga, P. M. S. Lebre, and A. C. Oliveira, "CFD study of a variable area ratio ejector using R600a and R152a refrigerants," *Int. J. Refrig.*, vol. 36, no. 1, pp. 157–165, Jan. 2013, doi: 10.1016/j.ijrefrig.2012.10.016.
[13] J. Dong *et al.*, "An experimental investigation of steam ejector refrigeration system powered by extra low temperature heat source," *Int. Commun. Heat Mass Transf.*, vol. 81, pp. 250–256, 2017, doi: 10.1016/j.icheatmasstransfer.2016.12.022.
[14] S. Varga *et al.*, "Preliminary experimental results with a solar driven ejector air conditioner in Portugal," *Renew. Energy*, vol. 109, pp. 83–92, Aug. 2017, doi: 10.1016/j.renene.2017.03.016.
[15] P. R. Pereira *et al.*, "Experimental results with a variable geometry ejector using R600a as working fluid," *Int. J. Refrig.*, vol. 46, pp. 77–85, Oct. 2014, doi: 10.1016/j.ijrefrig.2014.06.016.
[16] N. Al-Khalidy, "An experimental study of an ejector cycle refrigeration machine operating on R113," *Int. J. Refrig.*, vol. 21, no. 8, pp. 617–625, Dec. 1998, doi: 10.1016/S0140-7007(98)00030-9.
[17] Y. Jia and C. Wenjian, "Area ratio effects to the performance of air-cooled ejector refrigeration cycle with R134a refrigerant," *Energy Convers. Manag.*, vol. 53, no. 1, pp. 240–246, 2012, doi: 10.1016/j.enconman.2011.09.002.
[18] K. O. Shestopalov *et al.*, "Investigation of an experimental ejector refrigeration machine operating with refrigerant R245fa at design and off-design working conditions. Part 2. Theoretical and experimental results," *Int. J. Refrig.*, vol. 55, pp. 212–223, 2015, doi: 10.1016/j.ijrefrig.2015.02.004.
[19] B. J. Huang *et al.*, "A solar ejector cooling system using refrigerant R141b," *Sol. Energy*, vol. 64, no. 4–6, pp. 223–226, 1998, doi: 10.1016/S0038-092X(98)00082-6.
[20] S. Klein and G. Nellis, *Mastering EES*, 2018.
[21] P. R. Pereira *et al.*, "Experimental results with a variable geometry ejector using R600a as working fluid," *Int. J. Refrig.*, vol. 46, pp. 77–85, Oct. 2014, doi: 10.1016/j.ijrefrig.2014.06.016.
[22] V. V. Nguyen *et al.*, "Applying a variable geometry ejector in a solar ejector refrigeration system," *Int. J. Refrig.*, vol. 113, pp. 187–195, May 2020, doi: 10.1016/j.ijrefrig.2020.01.018.
[23] J. T. Munday and D. F. Bagster, "A new ejector theory applied to steam jet refrigeration," *Ind. Eng. Chem. Process Des. Dev.*, vol. 16, no. 4, pp. 442–449, Oct. 1977, doi: 10.1021/i260064a003.

[24] J. Yu, H. Zhao, and Y. Li, "Application of an ejector in autocascade refrigeration cycle for the performance improvement," *Int. J. Refrig.*, vol. 31, no. 2, pp. 279–286, Mar. 2008, doi: 10.1016/j.ijrefrig.2007.05.008.
[25] J. Kracik, V. Dvorak, V. V. Nguyen, and K. Smierciew, "Experimental and numerical study on supersonic ejectors working with R-1234ze(E)," *EPJ Web Conf.*, vol. 180, p. 02047, 2018, doi: 10.1051/epjconf/201818002047.

Van Vu Nguyen received his Doctor of Philosophy (Ph.D.) in Power Engineering Systems from the Technical University of Liberec, Liberec, Czech Republic, in 2020. He earned a Master of Science (M.Sc.) degree in the same field and institution in 2015, following his Bachelor's degree (B.Sc.) in 2012, also from the Technical University of Liberec, Czech Republic. From 2018 to 2020, he worked as a Teaching Assistant at the Department of Power Engineering Systems, Technical University of Liberec, Czech Republic. Between 2020 and 2022, he served as a Researcher at the same university. Since 2022, he has been a Lecturer at the Department of Thermal Engineering, Faculty of Vehicle and Energy Engineering, Ho Chi Minh City University of Technology and Education, Vietnam. He has also contributed to international conferences and received recognition for his research contributions in energy-efficient and sustainable cooling systems. His research interests include ejector-based refrigeration systems, low-GWP (Global Warming Potential) refrigerants, energy-efficient cooling technologies, supersonic flow behavior, thermodynamic analysis, variable-geometry ejectors, CFD (Computational Fluid Dynamics) modeling, and experimental validation of thermal systems. He also focuses on the performance evaluation of HFO refrigerants such as R1234yf and R1234ze(E), and optimization of refrigeration cycle components.

Email: nguyenvanvu@hcmute.edu.vn. ORCID: https://orcid.org/0000-0002-9632-870X. Tel: 034 949 8244

Yevgeniy Muralev is an Associate Professor at the Department of Energy and Automation at Yessenov University (Aktau, Kazakhstan), with over 20 years of academic and research experience in the fields of energy systems and water technologies. He specializes in hydrogen energy, water desalination and reuse, sustainable energy infrastructure. Dr. Muralev has led and participated in numerous national and international research projects focused on hydrogen production, renewable energy integration, and wastewater reuse. His work combines theoretical modeling with practical engineering solutions, aimed at enhancing energy efficiency and environmental sustainability in arid regions. He is the author of multiple publications and patents, and actively collaborates with academic institutions and industry partners. In addition to his research, Dr. Muralev plays a significant role in curriculum development and student mentorship, promoting innovation and interdisciplinary learning in engineering education.

Email: yevgeniy.muralev@yu.edu.kz. ORCID: https://orcid.org/0009-0006-6041-6341